

Designing an Improved Deep Learning-based Model for COVID-19 Recognition in Chest X-ray Images: A Knowledge Distillation Approach

AmirReza BabaAhmadi¹, Sahar Khalafi², Masoud ShariatPanahi³, Moosa Ayati⁴

Abstract

Background and Objectives: COVID-19 has adversely affected humans and societies in different aspects. Numerous people have perished due to inaccurate COVID-19 identification and, consequently, a lack of appropriate medical treatment. Numerous solutions based on manual and automatic feature extraction techniques have been investigated to address this issue by researchers worldwide. Typically, automatic feature extraction methods, particularly deep learning models, necessitate a powerful hardware system to perform the necessary computations. Unfortunately, many institutions and societies cannot benefit from these advancements due to the prohibitively high cost of high-quality hardware equipment. As a result, this study focused on two primary goals: first, lowering the computational costs associated with running the proposed model on embedded devices, mobile devices, and conventional computers; and second, improving the model's performance in comparison to previously published methods (at least performs on par with state of the art models) in order to ensure its performance and accuracy for the medical recognition task.

Methods: This study used two neural networks to improve feature extraction from our dataset: VGG19 and ResNet50V2. Both of these networks are capable of providing semantic features from the nominated dataset. Streaming in a fully connected classifier layer that feeds richer features, therefore feature vectors of these networks have been merged, and this action resulted in satisfactory classification results for normal and COVID-19 cases. On the other hand, these two networks have many layers and require a significant amount of computation. To this end, An alternative network was considered, namely MobileNetV2, which excels at extracting semantic features while requiring minimal computation on mobile and embedded devices. Knowledge distillation (KD) was used to transfer knowledge from the teacher network (concatenated ResNet50V2 and VGG19) to the student network (MobileNetV2) to improve MobileNetV2 performance and to achieve a robust and accurate model for the COVID-19 identification task from chest X-ray images.

Results: Pre-trained networks were used to provide a more useful starting point for the COVID-19 detection task. Additionally, a 5-fold cross-validation technique was used on both the teacher and student networks to evaluate the

¹ School of Mechanical Engineering, College of Engineering, University of Tehran, Tehran, Iran (email: babaahmadi.amir@ut.ac.ir)

² Department of Electrical and Computer Engineering, Isfahan University of Technology, Isfahan, Iran

³ School of Mechanical Engineering, College of Engineering, University of Tehran, Tehran, Iran

⁴ School of Mechanical Engineering, College of Engineering, University of Tehran, Tehran, Iran

proposed method's performance. Finally, the proposed model achieved 98.8% accuracy in detecting infectious and normal cases.

Conclusion: The study results demonstrate the proposed method's superior performance. With the student model achieving acceptable accuracy and F1-score using cross-validation technique, it can be concluded that this network is well-suited for conventional computers, embedded systems, and clinical experts' cell phones.

Keywords: COVID-19, Deep Learning, Medical Image Analysis, Knowledge Distillation, Chest X-ray images, Teacher-Student Model

1. Background and Objectives

COVID-19 has been a significant threat to human life and health in recent years. It has delivered a detrimental effect on healthcare systems worldwide. Unfortunately, COVID-19 is highly contagious and transmissible. As a result, it is inevitable to develop prediction systems capable of rapidly diagnosing it and averting its adverse effects. Numerous scientists have conducted multiple studies to develop human-level prediction and diagnosis systems to aid communities in combating this disease.

These methods are typically effective at detecting COVID-19 using CT and chest X-ray images. However, the fatal flaw is that automatic feature extraction techniques, particularly deep learning models, require a significant amount of computation to perform a specific task. Numerous hospitals and institutions are unable to procure expensive hardware systems capable of performing these algorithms.

Additionally, in the absence of medical experts, the health of the population in many developing countries may be jeopardized. In some developing countries, the scarcity of human experts capable of identifying medical diseases from medical images is a stark reality. As a result, an effort is made to offer an alternate solution to remedy this issue in this study.

This paper focuses on two primary objectives and charts the course accordingly: first, a fast algorithm capable of being deployed in conventional computers and embedded in mobile devices and tablets, and other embedded systems requires development. The second objective, which prompted developing a novel deep learning model, was to deliver more accurate and reliable results than previously published methods to ensure the algorithm's performance for medical diagnosis.

Recognizing COVID-19 is the first step toward treatment. The main objective of this paper is an attempt to address this step. COVID-19 is typically accompanied by symptoms including coughing, colds, and shortness of breath, among others. According to the WHO, respiratory problems are the fatal symptoms of COVID-19 and can be identified using CT scans or chest X-rays obtained in hospitals and medical clinics.

Deep learning and its associated techniques have been widely applied to computer vision tasks such as medical image analysis in recent years. Examples include tumor detection [1], diabetic retinopathy [2], among others.

Considering that medical image analysis is one of the most exciting applications of computer vision and deep learning, automatic feature extractor algorithms can be critical in diagnosing diseases at levels comparable to human experts. Due to the critical nature of the initial diagnosis, researchers have identified this step's accuracy as a significant challenge. The following section examines related works and studies in order to create a solid framework for our research. In [3], a model based on stacked convolutional neural networks with multiple pre-trained networks was proposed. In [4], a residual-layer-based neural network with a modified kernel was used to prognosticate the presence of COVID-19 in normal and pneumonia chest X-ray images.

[5] proposes a model based on an ensemble learning classifier to address the imbalance dataset issue. Another paper [6] introduced a combination of LSTM⁵ (for detection) and a convolutional neural network (for recognition). This method produced a 99.4% accuracy metric. [7] describes the development of a model using LSTM and GAN architectures. This method does not require the addition of a network for feature extraction for the binary classification task. [8] investigated the presence of COVID-19 in medical images using a deep neural network based on a CNN with additional components in different layers.

In [9], CNN and SVM⁶ were combined to analyze COVID-19 CXR images. [10] proposes a new framework based on the use of DarkNet53 to perform chest X-ray images. [11] conducted a comparative study to determine which model performs the best among pre-trained deep learning architectures. Fifteen models were examined in order to determine the optimal architecture. According to this study, VGG19 was the most accurate pre-trained model. Another comparative study [12] classified COVID-19 from normal cases and pneumonia using novel pre-trained architectures such as DenseNet 201, Inception V3, Resnet50, and a few other networks. [13] introduced a new model based on GAN and CNN. Multiple classifiers were used to perform the classification task in [13]. Furthermore, this paper developed a COVID-19 segmentation model using a unique dataset.

[14] compared pre-trained architectures and then modified those networks to reduce trainable parameters and enable faster algorithm training. [15] examined a variety of pre-trained architectures, including Alex-Net, VGG16, and the ResNet family. Moreover, this article concentrated on evaluating freezing layers and other configurations used in transfer learning methods. A study was conducted in [16] to determine the best candidate for COVID-19 recognition. Based on this research, the outstanding architecture for COVID-19 detection is achieved through the Inception Network. Another comparative study was conducted in [17] using DenseNet121, ResNet50, VGG16, and VGG19.

In [18], a binary classification task has been performed. Fine-tuning was performed on the final layer of the pre-trained SqueezeNet, DenseNet121, ResNet50, and ResNet18 networks. [19] depicts a voting-based procedure for evaluating

⁵ Long Short-Term Memory (LSTM)

⁶ Support Vector Machine (SVM)

VGG16, InceptionV3, and ResNet50 predictions. The final layer (output) compares the performance of all of the networks mentioned previously in a simultaneous manner and selects the best result.

In [20], an assessment of the effect of preprocessing on the results of CNN-based networks is made. [21] describes the development of a customized network dubbed COVID-Net for CXR and chest X-ray medical images. Another study [22] compared COVID-19, bacterial pneumonia, and viral-pneumonia classification results using state-of-the-art algorithms and CNN architecture. In another study [23], PCA⁷ was used to increase the efficiency of feature extraction. YOLO⁸ Networks with additional convolution layers involving modified kernels were used in [24] to detect COVID-19 from chest X-ray images.

[25] examined the performance of the Efficient-Net family in detecting COVID-19 and pneumonia in normal cases. In [26], a network, termed CoroNet, was introduced based on the Xception network to perform multi-class classification from normal category images, including pneumonia-viral, pneumonia-bacterial, and COVID-19.

This paper is structured as follows: The second section provides an overview of previous publications on the task. The third section describes the knowledge distillation method and explains why it was incorporated into the algorithm. Section four discusses the dataset that was used to conduct this research. Section five describes the training phase and the evaluation metrics. Finally, section six presents the proposed model's evaluation results, and section seven summarizes our paper's findings.

2. Methods

Nowadays, Deep Neural Networks⁹ have revolutionized the field of computer vision. Their applications have been extensively investigated in a variety of fields, including self-driving cars [27], medical image analysis [28][29], and agriculture [30], among others. CNNs¹⁰ have established themselves as the most effective tools for automatic feature extraction in computer vision and NLP¹¹, speech processing, and video classification tasks.

This paper demonstrates how CNN-based neural networks can improve semantic feature extraction for binary classification tasks involving COVID-19 and normal cases. DenseNet [31], ResNet [32], VGG [33], Xception [34], and Mobile-NetV2 [35] are some of the most powerful pre-trained networks. VGG19 is an extension of VGG16; it features sixteen convolutional layers and three fully connected layers. Five MaxPool layers are used, and the final layer is a SoftMax layer. ResNet50V2 is an enhanced version of ResNet50 that outperforms previous versions such as ResNet101.

⁷ Principal Component Analysis (PCA)

⁸ You Only Look Once (YOLO)

⁹ Deep Neural Networks (DNN)

¹⁰ Convolutional Neural Networks (CNN)

¹¹ Natural Language Processing (NLP)

ResNet50V2 has been equipped with several new connections between different blocks, allowing this network to achieve a high level of accuracy in the ImageNet competition. MobileNetV2 is a convolutional network designed with depth-wise convolution layers to improve accuracy while lowering computational costs. This reduction is caused by decreasing trainable parameters. Due to the use of inverted residual blocks, this network can be embedded in mobile phones, tablets, and other conventional embedded devices.

Since both ResNet50V2 and VGG19 generate the same size output layer (feature vector), their feature vectors were combined to produce a richer semantic feature set for the specified task. Afterward, a CNN layer was added to this architecture (kernel size 1 and 1024 filters). The network's output was then flattened and streamed into the fully connected layers. Notably, no activation function in the final CNN layer was used. The classification layer was constructed using 64 neurons in fully connected layers, with a dropout rate of 0.5. Another fully connected layer has been added to this layer, the final layer, whose neurons count is equal to the size of the problem's classes.

The entire architecture is termed the teacher network, with MobileNetV2 serving as the student network in a broader context referred to as the teacher-student model or knowledge distillation framework. The structure of the teacher model is depicted in Figure 1. The tensors' feature size for both ResNet50V2 and VGG19 is $10 \times 10 \times 2048$, and the size of the concatenated feature is $10 \times 10 \times 4096$.

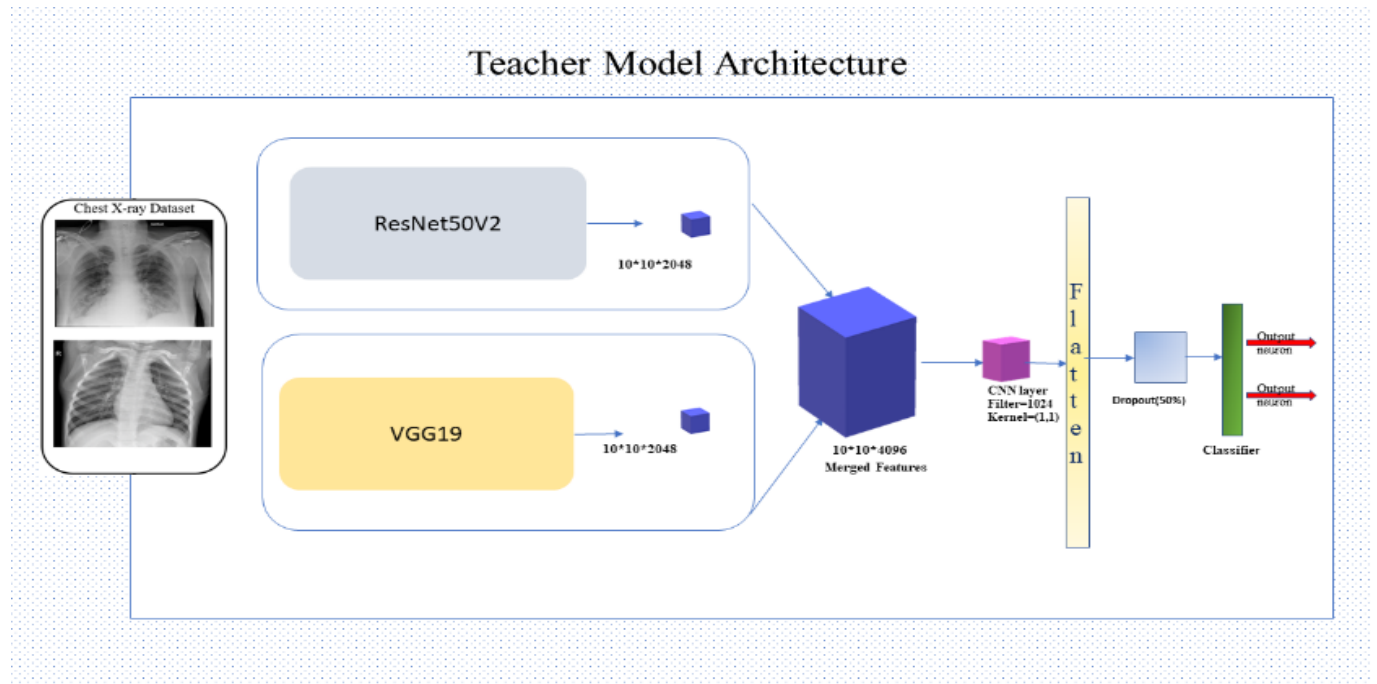


Figure 1. Teacher Model Architecture

3. Knowledge Distillation

Hinton et al. pioneered Knowledge Distillation¹² in [36]. KD is a process that involves training a smaller network to imitate the behavior of a more extensive network. The purpose of designing a complex network as a teacher is to learn more sophisticated features and deliver better results. However, we typically want to run our network on a standard computer or embedded device.

Due to the limitation of memory size and computational cost, frequent issues arise. As a result, a solution is required to address these issues. A weighted average (mean) is necessary to distill knowledge from teacher to student. Cross-Entropy with soft targets is the initial objective function. Through the softmax function in the smaller network, this objective function is calculated based on high temperature. A more significant architecture (network) must be used to generate soft targets. Cross-Entropy with valid labels is the second objective function. This function is calculated using the softmax output from the student model by setting the temperature to zero.

The teacher network and the student network begin receiving training data in parallel. The teacher model contains a softmax with temperature in its output. By contrast, the student model generates two different outputs. The first output is softmax with temperature, while the second output contains standard softmax. The student model is intended to produce softened probabilities (the output of the teacher model). The following formula is used to calculate the loss of knowledge distillation:

$$L_{KD} = \alpha KL(p,q)T^2 + (1 - \alpha)L(W_s,x) \quad (1)$$

Where p and q denote the probabilities generated by student and teacher networks in a specific temperature (T), respectively, and KL denotes the Kullback-Leibler divergence, which measures the level of distinction between two probabilistic distributions. The Cross-Entropy of the student model with $T=1$ is (LW_s,x) . According to [36], α and T are hyperparameters where the greater the value of α , the better the learning experience for the student model.

Back-propagation must be performed only in the student network during the distillation phase to add a significant element to this description since the teacher has already tuned its parameters. The teacher's knowledge is then transferred to the student model throughout the distillation procedure. Notably, the student model can be trained at a faster rate than the teacher model. For more details regarding the distillation procedure, please refer to [37]. The procedure for knowledge distillation is depicted in Figure 1.

¹² Knowledge Distillation (KD)

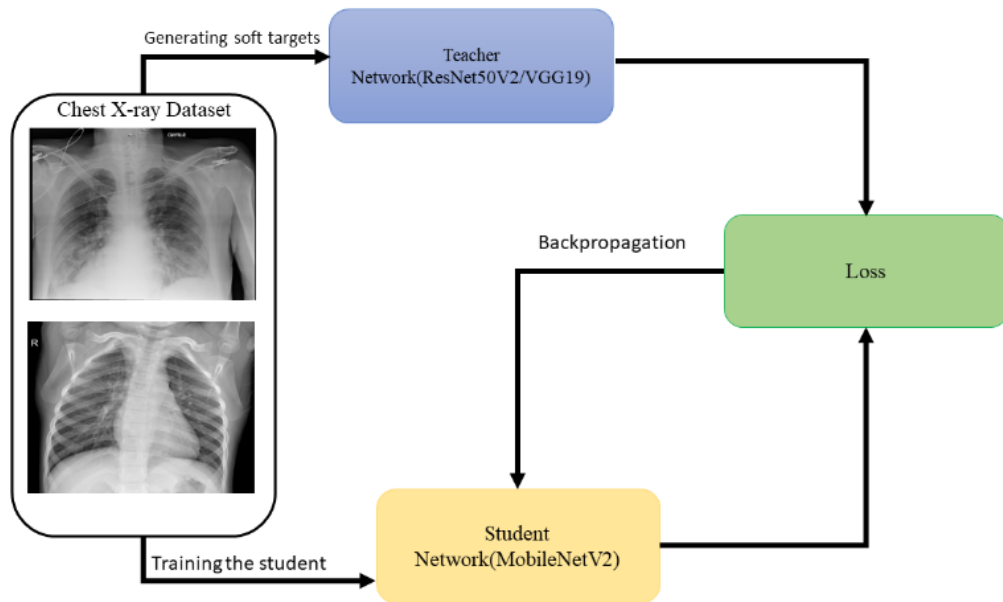


Figure 2. Knowledge Distillation for COVID-19 detection

4. Dataset

Two public datasets were used to train the proposed deep learning model to build the required dataset. First, a public dataset available at (<https://github.com/ieee8023/covid-chestxray-dataset>) was used for positive samples of COVID-19. Afterward, the dataset available at (<https://www.kaggle.com/c/rsna-pneumonia-detection-challenge>) was used to collect negative samples (normal cases).

Following the two datasets being merged, 118 COVID-19 cases and 8851 normal cases were established. It became clear that an unbalanced dataset was created due to the number of positive cases (COVID-19) being significantly lower than the number of normal chest X-ray medical images. As a result, the issue was mitigated through the use of sampling techniques. The central concept is to select an equal number of items from each category for the binary classification task. The oversampling method was used to increase COVID-19 (positive cases) samples to ensure that both positive and negative classes had an equal number of samples.

The number of positive cases increased to 8851 following the oversampling technique, while the number of negative (normal) samples remained unchanged. It should be noted that no images of pneumonia were used in this study. Pneumonia is classified into several different classes, including SARS, Streptococcus, ARDS, and Pneumocystis. In this respect, treating all of these categories as a single class was deemed as impractical. This cannot be very clear in terms of interpreting recognition task results as distinct pneumonia types require a unique type of treatment. As a result, developing a pneumonia-type classifier was deferred to a later date. Figure 3 illustrates a selection of patients with COVID-19 and normal images from the dataset.



Figure 3(a): Healthy person



Figure 3(b): Patient with COVID-19

4.1 Data Augmentation

Before data augmentation, the images were normalized to avoid issues with vanishing and exploding gradients. After that, the image was resized to 224x224. The model was then enhanced with data augmentation techniques to make it more responsive to variations within the medical images. During data augmentation, it was assumed that variations in the images did not affect the label's (ground truth) definition. Random rotation was the only data augmentation

approach considered for the dataset, between (0-20⁰). This can prevent overfitting and also helps the learning curve converge more quickly.

5. Training Phase

The training phase consumed approximately 80% of the dataset, with the remaining 20% used for the test phase. The K-fold Cross-Validation technique was used to ensure the accuracy of the performance evaluation. The loss function was binary Cross-Entropy, and the optimizer was Adam (with a learning rate=1e-5). The number of folds was 5 (k=5). The batch size was 32, and the epoch number was set to 120.

5.1 Evaluation Metrics

Several specific criteria need to be established for evaluating the model's performance on the test dataset. True Positive refers to correctly identifying COVID-19 positives among both positive and normal cases. In the conceptualization, true negativity entails accurately identifying normal cases. False Positive refers to the practice of misdiagnosing COVID-19 cases as normal. False-negative prediction is misclassifying normal cases as COVID-19 cases.

Precision is defined as the ratio of True Positives over the sum of True Positives and False Positives.

$$Precision = \frac{TP}{TP + FP} \quad (1)$$

Sensitivity is the ratio of True Positives over to the sum of True Positives and False Negatives.

$$Sensitivity(recall) = \frac{TP}{TP + FN} \quad (2)$$

Specificity is the ratio of True Negatives over the sum of False Positives and True Negatives.

$$Specificity = \frac{TN}{TN + FP} \quad (3)$$

Finally, three additional criteria were used to measure the performance of the proposed model on the study's dataset (F1 Score and Balanced-Accuracy in addition to conventional accuracy).

$$F1-Score = \frac{2 * precision * recall}{(precision + recall)} \quad (4)$$

$$Balanced\ Accuracy = \frac{specificity + sensitivity}{2} \quad (5)$$

$$Accuracy = \frac{TP + TN}{Positive + Negative} \quad (6)$$

6. Results and Discussion

In this section, we present the results of our method applied to the dataset mentioned above. The images which have been used for the test have not been seen before by the algorithm. Therefore, these results are approvable that the proposed algorithm can perform very well on unseen medical images. Table 1 presents the results of the training teacher model. It is conspicuous that the teacher's performance is enough to detect chest X-ray images with good accuracy and F1-score. Table 2 shows the results of MobileNetV2 (student model). Its results are satisfactory for the classification task. Despite presenting good results of the student network, we decided to improve its classification ability via the knowledge distillation approach. Table 3 is presenting the results of the student network after knowledge distillation is completed. Eventually, the student network performs on par with the existing methods in the literature and sometimes achieves better accuracy and F1-score in comparison with previous publications.

Table 1: Evaluation results of the Teacher Network (ResNet50V2/VGG19)

| Fold No. | Acc | Precision | Specificity | Recall(sensitivity) | F1 score | Balanced-Acc |
|----------------|--------------|--------------|--------------|---------------------|--------------|--------------|
| 1 | 0.978 | 0.978 | 0.978 | 0.978 | 0.978 | 0.978 |
| 2 | 0.989 | 0.978 | 1.000 | 1.000 | 0.988 | 1.000 |
| 3 | 1.000 | 1.000 | 1.000 | 1.000 | 1.000 | 1.000 |
| 4 | 0.989 | 0.978 | 1.000 | 1.000 | 0.988 | 1.000 |
| 5 | 1.000 | 1.000 | 1.000 | 1.000 | 1.000 | 1.000 |
| Average | 0.992 | 0.987 | 0.996 | 0.996 | 0.991 | 0.996 |

Table 2: Evaluation results of the Student Network (MobileNetV2) *Before* Knowledge-Distillation

| Fold No. | Acc | Precision | Specificity | Recall(sensitivity) | F1 score | Balanced-Acc |
|----------------|--------------|--------------|--------------|---------------------|--------------|--------------|
| 1 | 0.987 | 0.978 | 1.000 | 1.000 | 0.992 | 1.000 |
| 2 | 0.974 | 0.976 | 0.976 | 0.976 | 0.972 | 0.976 |
| 3 | 0.974 | 0.976 | 0.976 | 0.976 | 0.972 | 0.976 |
| 4 | 0.987 | 0.978 | 1.000 | 1.000 | 0.992 | 1.000 |
| 5 | 0.987 | 0.978 | 1.000 | 1.000 | 0.992 | 1.000 |
| Average | 0.980 | 0.977 | 0.990 | 0.990 | 0.984 | 0.990 |

Table 3: Evaluation results of the Student Network (MobileNetV2) *After* Knowledge-Distillation

| Fold No. | Acc | Precision | Specificity | Recall(sensitivity) | F1 score | Balanced-Acc |
|---------------------|--------------|--------------|--------------|---------------------|--------------|--------------|
| 1 | 0.974 | 0.976 | 0.976 | 0.976 | 0.972 | 0.976 |
| 2 | 1.000 | 1.000 | 1.000 | 1.000 | 1.000 | 1.000 |
| 3 | 0.978 | 0.978 | 1.000 | 1.000 | 0.992 | 1.000 |
| 4 | 1.000 | 1.000 | 1.000 | 1.000 | 1.000 | 1.000 |
| 5 | 0.989 | 0.978 | 1.000 | 1.000 | 0.988 | 1.000 |
| Average | 0.988 | 0.987 | 0.996 | 0.996 | 0.991 | 0.996 |
| %Improvement | 0.8 % | 1.0 % | 0.6 % | 0.6 % | 0.7 % | 0.6 % |

Table 4: Number of total parameters in each architecture

| | |
|---|----------------|
| Teacher Network (ResNet50V2/VGG19) | 49,222,390 |
| Student Network (MobileNetV2) | 2,334,966 |
| Number of Parameters Reduction (%) | -95.3 % |

It is noteworthy that the student network has outperformed its previous version(without KD) in terms of evaluation metrics performance, and this is because knowledge distillation improves MobileNetV2's performance to some extent. Meanwhile, KD aids the network in mitigating common neural network forgetting problems. Thus, the student model's performance demonstrates that it can be used for medical recognition tasks in embedding systems while requiring minimal computation, owing to the use of depthwise convolutional layers and knowledge distillation. Table 4 shows the number of parameters in each architecture. It's conspicuous that not only KD can improve student model's performance, but also it reduces the number of parameters about 95.3% while maintaining performance. Therefore, student model can be an eligible candidate for COVID-19 recognition task.

7. Conclusion

In this paper, a novel method was developed for identifying COVID-19 medical chest X-ray images. Due to encountering an unbalanced dataset, this issue was resolved using oversampling and data augmentation techniques. In evaluating the algorithm, the fivefold cross-validation method was used to ensure the proposed model's performance. After performing knowledge distillation, an accuracy and F1-score of 98.8% and 99.1% were achieved respectively. The proposed method, we believe, is an excellent choice for the COVID-19 recognition task. However, adding more diverse datasets from different countries will help improve the algorithm. For future works on medical image datasets, incremental learning techniques, self-supervised deep learning methods, vision transformer architectures, knowledge distillation under adversarial attacks are proposed.

Declaration

Conflict of interest

The corresponding author declares that there are no conflicts of interest on behalf of all authors.

References

- [1] K. Paeng, S. Hwang, S. Park, and M. Kim, "A unified framework for tumor proliferation score prediction in breast histopathology," in *Lecture Notes in Computer Science (including subseries Lecture Notes in Artificial Intelligence and Lecture Notes in Bioinformatics)*, 2017, vol. 10553 LNCS, pp. 231–239, doi: 10.1007/978-3-319-67558-9_27.
- [2] J. de la Torre, A. Valls, and D. Puig, "A deep learning interpretable classifier for diabetic retinopathy disease grading," *Neurocomputing*, vol. 396, pp. 465–476, Jul. 2020, doi: 10.1016/J.NEUCOM.2018.07.102.
- [3] A. Gupta, Anjum, S. Gupta, and R. Katarya, "InstaCovNet-19: A deep learning classification model for the detection of COVID-19 patients using Chest X-ray," *Appl. Soft Comput.*, vol. 99, Feb. 2021, doi: 10.1016/J.ASOC.2020.106859.
- [4] C. Ouchicha, O. Ammor, and M. Meknassi, "CVDNet: A novel deep learning architecture for detection of coronavirus (Covid-19) from chest x-ray images," *Chaos, Solitons and Fractals*, vol. 140, Nov. 2020, doi: 10.1016/J.CHAOS.2020.110245.

- [5] P. Saha, M. S. Sadi, and M. M. Islam, "EMCNet: Automated COVID-19 diagnosis from X-ray images using convolutional neural network and ensemble of machine learning classifiers," *Informatics Med. Unlocked*, vol. 22, Jan. 2021, doi: 10.1016/J.IMU.2020.100505.
- [6] M. Z. Islam, M. M. Islam, and A. Asraf, "A combined deep CNN-LSTM network for the detection of novel coronavirus (COVID-19) using X-ray images," *Informatics Med. Unlocked*, vol. 20, Jan. 2020, doi: 10.1016/J.IMU.2020.100412.
- [7] S. Sheykhivand *et al.*, "Developing an efficient deep neural network for automatic detection of COVID-19 using chest X-ray images," *Alexandria Eng. J.*, vol. 60, no. 3, pp. 2885–2903, Jun. 2021, doi: 10.1016/J.AEJ.2021.01.011.
- [8] E. Hussain, M. Hasan, M. A. Rahman, I. Lee, T. Tamanna, and M. Z. Parvez, "CoroDet: A deep learning-based classification for COVID-19 detection using chest X-ray images," *Chaos, Solitons and Fractals*, vol. 142, Jan. 2021, doi: 10.1016/J.CHAOS.2020.110495.
- [9] Y. KUTLU and Y. CAMGÖZLÜ, "Detection of coronavirus disease (COVID-19) from X-ray images using deep convolutional neural networks," *Nat. Eng. Sci.*, vol. 6, no. 1, pp. 60–74, Jan. 2021, doi: 10.28978/NESCIENCES.868087.
- [10] R. C. Joshi *et al.*, "A deep learning-based COVID-19 automatic diagnostic framework using chest X-ray images," *Biocybern. Biomed. Eng.*, vol. 41, no. 1, pp. 239–254, Jan. 2021, doi: 10.1016/J.BBE.2021.01.002.
- [11] M. M. Rahaman *et al.*, "Identification of COVID-19 samples from chest X-Ray images using deep learning: A comparison of transfer learning approaches," *J. Xray. Sci. Technol.*, vol. 28, no. 5, pp. 821–839, 2020, doi: 10.3233/XST-200715.
- [12] K. El Asnaoui and Y. Chawki, "Using X-ray images and deep learning for automated detection of coronavirus disease," *J. Biomol. Struct. Dyn.*, pp. 1–12, 2020, doi: 10.1080/07391102.2020.1767212.
- [13] M. Loey, F. Smarandache, and N. E. M. Khalifa, "Within the lack of chest COVID-19 X-ray dataset: A novel detection model based on GAN and deep transfer learning," *Symmetry (Basel)*, vol. 12, no. 4, Apr. 2020, doi: 10.3390/SYM12040651.
- [14] R. K. Singh, R. Pandey, and R. N. Babu, "COVIDScreen: explainable deep learning framework for differential diagnosis of COVID-19 using chest X-rays," *Neural Comput. Appl.*, 2021, doi: 10.1007/S00521-020-05636-6.
- [15] S. Sarv Ahrabi, M. Scarpiniti, E. Baccarelli, and A. Momenzadeh, "An accuracy vs. Complexity comparison of deep learning architectures for the detection of covid-19 disease," *computation*, vol. 9, no. 1, pp. 1–20, Jan. 2021, doi: 10.3390/COMPUTATION9010003.

- [16] I. Lorencin *et al.*, "Automatic evaluation of the lung condition of COVID-19 patients using X-ray images and convolutional neural networks," *J. Pers. Med.*, vol. 11, no. 1, pp. 1–31, Jan. 2021, doi: 10.3390/JPM11010028.
- [17] R. Jain, M. Gupta, S. Taneja, and D. J. Hemanth, "Deep learning-based detection and analysis of COVID-19 on chest X-ray images," *Appl. Intell.*, vol. 51, no. 3, pp. 1690–1700, Mar. 2021, doi: 10.1007/S10489-020-01902-1.
- [18] S. Minaee, R. Kafieh, M. Sonka, S. Yazdani, and G. Jamalipour Soufi, "Deep-COVID: Predicting COVID-19 from chest X-ray images using deep transfer learning," *Med. Image Anal.*, vol. 65, Oct. 2020, doi: 10.1016/J.MEDIA.2020.101794.
- [19] S. C. R and R. K. Dubey, "Deep Learning-Based Hybrid Models for Prediction of COVID-19 using Chest X-Ray," Aug. 2020, doi: 10.36227/TECHRXIV.12839204.V1.
- [20] J. D. Arias-Londono, J. A. Gomez-Garcia, L. Moro-Velazquez, and J. I. Godino-Llorente, "Artificial Intelligence applied to chest X-Ray images for the automatic detection of COVID-19. A thoughtful evaluation approach," *IEEE Access*, 2020, doi: 10.1109/ACCESS.2020.3044858.
- [21] L. Wang, Z. Q. Lin, and A. Wong, "COVID-Net: a tailored deep convolutional neural network design for detection of COVID-19 cases from chest X-ray images," *Sci. Rep.*, vol. 10, no. 1, Dec. 2020, doi: 10.1038/S41598-020-76550-Z.
- [22] I. D. Apostolopoulos and T. A. Mpesiana, "Covid-19: automatic detection from X-ray images utilizing transfer learning with convolutional neural networks," *Phys. Eng. Sci. Med.*, vol. 43, no. 2, pp. 635–640, Jun. 2020, doi: 10.1007/S13246-020-00865-4.
- [23] T. Garg, M. Garg, O. P. Mahela, and A. R. Garg, "Convolutional Neural Networks with Transfer Learning for Recognition of COVID-19: A Comparative Study of Different Approaches," *AI*, vol. 1, no. 4, pp. 586–606, Dec. 2020, doi: 10.3390/AI1040034.
- [24] T. Ozturk, M. Talo, E. A. Yildirim, U. B. Baloglu, O. Yildirim, and U. Rajendra Acharya, "Automated detection of COVID-19 cases using deep neural networks with X-ray images," *Comput. Biol. Med.*, vol. 121, Jun. 2020, doi: 10.1016/J.COMPBIOMED.2020.103792.
- [25] E. Luz *et al.*, "Towards an effective and efficient deep learning model for COVID-19 patterns detection in X-ray images," *Res. Biomed. Eng.*, Apr. 2021, doi: 10.1007/S42600-021-00151-6.
- [26] A. I. Khan, J. L. Shah, and M. M. Bhat, "CoroNet: A deep neural network for detection and diagnosis of COVID-19 from chest x-ray images," *Comput. Methods Programs Biomed.*, vol. 196, Nov. 2020, doi: 10.1016/J.CMPB.2020.105581.

- [27] C. Häne *et al.*, "3D visual perception for self-driving cars using a multi-camera system: Calibration, mapping, localization, and obstacle detection," *Image Vis. Comput.*, vol. 68, pp. 14–27, Dec. 2017, doi: 10.1016/J.IMAVIS.2017.07.003.
- [28] X. Qiu, Z. Liu, M. Zhuang, D. Cheng, C. Zhu, and X. Zhang, "Fusion of CNN1 and CNN2-based Magnetic Resonance Image Diagnosis of Knee Meniscus Injury and a Comparative Analysis with Computed Tomography," *Comput. Methods Programs Biomed.*, p. 106297, Jul. 2021, doi: 10.1016/J.CMPB.2021.106297.
- [29] C. Liao, C. Wang, J. Bai, L. Lan, and X. Wu, "Deep learning for registration of region of interest in consecutive wireless capsule endoscopy frames," *Comput. Methods Programs Biomed.*, vol. 208, p. 106189, Sep. 2021, doi: 10.1016/J.CMPB.2021.106189.
- [30] C. Ren, D. K. Kim, and D. Jeong, "A Survey of Deep Learning in Agriculture: Techniques and Their Applications," *J. Inf. Process. Syst.*, vol. 16, no. 5, pp. 1015–1033, 2020, doi: 10.3745/JIPS.04.0187.
- [31] G. Huang, Z. Liu, L. van der Maaten, and K. Q. Weinberger, "Densely Connected Convolutional Networks," *Proc. - 30th IEEE Conf. Comput. Vis. Pattern Recognition, CVPR 2017*, vol. 2017-January, pp. 2261–2269, Aug. 2016, Accessed: Jul. 26, 2021. [Online]. Available: <https://arxiv.org/abs/1608.06993v5>.
- [32] K. He, X. Zhang, S. Ren, and J. Sun, "Deep residual learning for image recognition," in *Proceedings of the IEEE Computer Society Conference on Computer Vision and Pattern Recognition*, Dec. 2016, vol. 2016-December, pp. 770–778, doi: 10.1109/CVPR.2016.90.
- [33] K. Simonyan and A. Zisserman, "Very deep convolutional networks for large-scale image recognition," Sep. 2015, Accessed: Jun. 17, 2021. [Online]. Available: <http://www.robots.ox.ac.uk/>.
- [34] F. Chollet, "Xception: Deep learning with depthwise separable convolutions," in *Proceedings - 30th IEEE Conference on Computer Vision and Pattern Recognition, CVPR 2017*, Nov. 2017, vol. 2017-January, pp. 1800–1807, doi: 10.1109/CVPR.2017.195.
- [35] M. Sandler, A. Howard, M. Zhu, A. Zhmoginov, and L. C. Chen, "MobileNetV2: Inverted Residuals and Linear Bottlenecks," in *Proceedings of the IEEE Computer Society Conference on Computer Vision and Pattern Recognition*, Dec. 2018, pp. 4510–4520, doi: 10.1109/CVPR.2018.00474.
- [36] G. Hinton, O. Vinyals, and J. Dean, "Distilling the Knowledge in a Neural Network," Mar. 2015, Accessed: Jul. 26, 2021. [Online]. Available: <https://arxiv.org/abs/1503.02531v1>.
- [37] J. Gou, B. Yu, S. J. Maybank, and D. Tao, "Knowledge Distillation: A Survey," *Int. J. Comput. Vis.*, vol. 129, no. 6, pp. 1789–1819, Jun. 2020, doi: 10.1007/s11263-021-01453-z.